



Research Article

Development of a Two-Compartment System *In vitro* Dissolution Test and Correlation with *In vivo* Pharmacokinetic Studies for Celecoxib

Shan Jiang,¹ Guoqing Zhang,¹ Lei Wang,¹ Ye Zeng,¹ Wenjie Liu,¹ and Zeneng Cheng^{1,2}

Received 4 September 2019; accepted 14 December 2019; published online 7 January 2020

Abstract. The objective of this study was to develop a novel open-mode two-compartment system dissolution apparatus to simulate the dissolution and absorption of poorly soluble drugs and to establish an *in vitro-in vivo* correlation (IVIVC). Celecoxib (CEB) was selected as a model drug, and *in vitro* dissolution was performed using the novel dissolution apparatus with acetate buffers at pH 4.5 containing Tween 80 (0.15%, w/v), at a flow rate of 30 mL/min and an agitation rate of 50 rpm. Cumulative release of all formulations was incomplete at approximately 70–80%, which likely reflected *in vivo* dissolution. Corresponding pharmacokinetic studies were performed in which twelve healthy male subjects from two bioequivalence studies received either one immediate release (IR) dose of the test (test 1 or test 2) or the reference formulation (Celebrex®, 200 mg). Individual plasma profiles of the formulations were deconvoluted *via* the Wanger-Nelson method to obtain the mean absorption fractions. A level A correlation was successfully developed with a good R². The Weibull equation was used to describe the *in vitro* dissolution and *in vivo* absorption kinetics. *In vitro* dissolution correlated with *in vivo* absorption was applied successfully to predict the *in vivo* plasma concentrations-time profiles of the CEB formulations. Compared with conventional methods, the novel dissolution device showed great potential for discriminating the dissolution between formulations and generic drugs, which may provide a tool for making *in vivo* predictions for next bioequivalence trials.

KEY WORDS: open-mode two-compartment system; celecoxib; bioequivalence; IVIVC; Weibull function.

INTRODUCTION

In recent years, the concept and applications of the *in vitro-in vivo* correlation (IVIVC) for oral drugs in solid forms have raised concerns in the pharmaceutical industry, academia, and regulatory departments (1,2). According to the Food and Drug Administration (FDA), IVIVC describes the mathematical model that allows *in vitro* drug characteristics to conform to its *in vivo* biological characteristics, for instance, from *in vitro* drug release to the relevant *in vivo*

response such as plasma drug concentration or drug absorption (3). When an IVIVC is established, the *in vitro* dissolution value can provide a key link to predict *in vivo* drug characteristics and serving as a surrogate for *in vivo* bioequivalence (BE) studies, potentially supporting a biowaiver, which could save cost and time in clinical trials (4–6).

In vivo dissolution is the process of drug dissolution in the gastrointestinal tract (7). For Biopharmaceutics Classification System (BCS) Class II drugs with poor water solubility and high permeability, dissolution is the rate-limiting step for absorption, which is probable to establish an IVIVC (8).

Ideally, *in vitro* tests should closely simulate the rate-limiting step for *in vivo* drug release. Dissolution conditions primarily simulate the gastrointestinal environment, including the pH value, enzymes, surface tension, gastric fluid volume, and temperature. Although the gastrointestinal environment is simulated by choosing different dissolution devices and media for *in vitro* dissolution tests, conventional dissolution testing methods often exhibit poor predictive ability for *in vivo* performance. For example, the basket, paddle, and reciprocating cylinder apparatus described in the United States Pharmacopeia (USP) are the most frequent dissolution

Electronic supplementary material The online version of this article (<https://doi.org/10.1208/s12249-019-1612-8>) contains supplementary material, which is available to authorized users.

¹Xiangya School of Pharmaceutical Science, Central South University, 172 Tongzipo Road, Changsha, 410013, Hunan, China.

²To whom correspondence should be addressed. (e-mail: chengzn@csu.edu.cn)

Abbreviations: (IVIVC), *In vitro-in vivo* correlation; (CEB), Celecoxib; (BE), Bioequivalent; (BCS), Biopharmaceutics Classification System; (HPLC), High-performance liquid chromatography; (FDA), Food and Drug Administration; (SDS), Sodium dodecyl sulfate.

methods (9,10). However, these dissolution devices have some shortcomings. One is that the basket and paddle apparatuses are a one-compartment, closed dissolution system which cannot simulate the continuous dynamic characteristics *in vivo* and lack absorptive sink conditions (11). Moreover, the basket/paddle methods are still widely used to investigate drug release and solubility except for absorbability under a defined solvent volume and high-level surfactants conditions (for poorly water-soluble drugs). These methods deviate from *in vivo* conditions and conceal the dissolution differentiation between pharmaceutical preparations (12). Thus, the *in vitro* dissolution tests cannot truly reflect the actual dissolution behavior *in vivo* and often fail to predict drug absorbability (13). Conventional dissolution tests have remained unable to meet this need primarily because of the lack of a biological correlation. Artificial stomach-duodenum models (14), dissolution-permeation models (15), and biphasic dissolution model have been proposed. In particular, biphasic dissolution systems consisted of an aqueous buffer and a water-insoluble organic solvent attract many interests. Shi *et al.* applied a biphasic dissolution system to examine release profiles of celecoxib formulations (a Celebrex® capsule, a drug solution containing surfactant and a self-emulsifying drug delivery system) (16). However, the use of an organic solvent and lack of a physical barrier between the two phases limits its applicability (17). Studies that examine that ability to discriminate differences within the same dosage forms are lacking.

Herein, considering the theory of drug dissolution and drug absorption, combined with the characteristics of biopharmaceutics, a novel open-mode two-compartment system dissolution apparatus was developed to reflect drug dissolution or absorption *in vivo* by controlling the dissolution *in vitro*. The novel device had two major advantages compared with single aqueous phase systems. First, two-compartment device consists of the donor compartment and the acceptor compartment, which can maintain absorptive sink conditions in the absence of high-level surfactants, because the dissolved drugs are continuously removed. This enabled reducing accumulation of dissolved drugs found in the single aqueous phase system. Second, two-compartment device enables using multiple media, including a pH shift and the different surfactant concentrations during the same experiments to simulate the real dissolution conditions and *in vivo* performance in the gastrointestinal tract. This provides a unique application advantages in establishing an IVIVC of drugs. Different dissolution media could be changed at different time intervals using a solvent selector from the media reservoir. For example, dissolution media could be started at acidic conditions (pH 1.2) and shifted to more basic pH values to simulate the gastric dissolution followed by intestinal dissolution and absorption. In addition, the device has an agitation function to reduce the adhesion of insoluble drugs with high amounts of active pharmaceutical ingredients compared with the flow-through cell method in the presence of vertical media flow shear stress and the absence of transversal shearing force. The large cross-sectional filtration area enables removing insoluble or sticky drugs or excipient granules that blocked the filter and created backpressure into the flow-through cell (18).

Celecoxib (CEB, trade name Celebrex®), a selective cyclooxygenase 2 (COX-2) inhibitor, has a good effect on treatment of osteoarthritis, rheumatoid arthritis, and acute pain (16), which was selected as a model drug. CEB is weakly acidic with a pKa of 11.1 (19), and is also characterized as a BCS class II drug owing to its low aqueous solubility (~ 5 µg/mL in water) and good permeability with a LogP of 3.5 (20,21). In this context, the purpose of this study was to develop an IVIVC using an open-mode two-compartment device for three celecoxib oral immediate-release (IR) formulations, including the reference product (Celebrex®), and two generic formulations (test 1 and test 2). A novel dissolution method combining BE studies was used to establish a good IVIVC with a discriminative dissolution method *in vitro*.

MATERIALS AND METHODS

Materials

Tween 80, sodium lauryl sulfate (SDS), sodium acetate, acetic acid, and sodium phosphate were purchased from Sin Pharm Chemical Reagent Co., Ltd. (Shanghai, China). Capsules for test 1 and test 2 were provided by two pharmaceutical companies. Commercial celecoxib capsules (Celebrex®, specifications: 200 mg, Pfizer, USA) were purchased from a pharmacy. The formulation was composed of croscarmellose sodium, edible inks, gelatin, lactose monohydrate, magnesium stearate, povidone, and sodium lauryl sulfate. The content of SDS in test 1 and test 2 was different.

Acetonitrile and other chemicals used met ACS reagent or USP/NF specifications. Ultrapure water from a laboratory water purification system (Hitech Instruments Co., Ltd., Shanghai, China) was used in all experimental procedures.

In vitro Dissolution

Device Description and Procedure

The core of the novel dissolution apparatus provided an open-mode two-compartment system. The five parts of device were the liquid delivery system, donor compartment, acceptor compartment, sample collection system, and temperature control system, which were assembled into an integrated apparatus through the shell structure (Fig. 1). For the two-compartment system, the donor compartment was an inner chamber, porous, 125-mL cup (3.5 cm in diameter and 10 cm in height) wrapped with a 0.45-µm filter membrane. The acceptor compartment was an outer chamber 250-mL cup. The donor compartment was placed into the acceptor compartment with a 1-cm dimension of gap and was connected *via* the 1200-mesh (11 µm) permeation holes. The medium volume of the new device ranged from 100 to 250 mL (the two-compartment total volume was 250 mL with a 1:1 ratio, half of the outer cup would diffuse into the inner cup). Less solvent volumes satisfied formulations with low amounts of active pharmaceutical ingredients. This was similar to the actual liquid volume of the gastrointestinal tract (22,23), and mimicked the sink conditions of the gastrointestinal tract containing surfactants such as bile salts

(16). Moreover, there was a dual filtration system between the donor and acceptor compartment. The primary filtration was displayed *via* an inner porous cup with 1200-mesh pore size and the externally wrapped with cellulose esters filter membrane served as a dual filtration function. Thus, the large filtration area resolved the problem of pipeline blockage (24). The rotating basket was used as a dosage form holder to provide mechanical agitation. The device operation procedure was as follows. The media inlet was connected to the media storage bottle and delivered into the donor compartment at a determined flow rate using a high-precision liquid inlet pump (Baoding Shenchen Precision Pump Co., Ltd., China). Meanwhile, the media and dissolved drug diffused from the donor compartment to the acceptor compartment were filtered thoroughly and was removed *via* the sampling needle. The flow rate varied from 0.5–50 mL/min through the main path of liquid discharge to the three-way valve, which separated two discharge branches and connected to the sample collector or the waste collection bottle to compose the dissolution-absorption process.

Dissolution Tests Using the Two-Compartment System Device

Dissolution assays in the novel apparatus were performed in acetate buffers at pH 4.5 containing Tween 80 (0.15% W/V) and the temperature was maintained at $37.0 \pm 0.5^\circ\text{C}$. The solution flow rate was 30 mL/min, the dissolution volume was 150 mL, and the basket stirring speed was fixed at 50 rpm. Samples (2 mL) were collected from the acceptor compartment at regular time intervals (5, 10, 15, 20, 25, 30, 35, 40, 45, 50, 60, 70, 80, 90, 100, 110, 120, and 150 min). Celecoxib was detected using the high-performance liquid chromatography (HPLC) on a TC-C18 column (5 μm , 4.6×150 mm, Agilent, USA) at 30°C . The mobile phase consisted of acetonitrile and water (55:45, v/v) with the flow rate at 1.0 mL/min. The injection volume was 10 μL and the detection wavelength was set at 254 nm. At least six capsules were tested per run.

Single-Phase Dissolution Tests Under Sink Conditions and Non-sink Conditions

Single-phase dissolution tests were performed under sink conditions and non-sink conditions to compare them with the novel methods. Per the US pharmacopeia, dissolution tests under sink conditions were carried out using the USP apparatus II (paddles) method (1000 mL, 0.04 mol/L tribasic sodium phosphate solution at pH 12 containing 1.0% SDS, at 50 rpm). Dissolution tests under non-sink conditions were performed using paddle methods (1000 mL acetate buffer at pH 4.5 containing 0.15% Tween 80 with a stirring speed of 50 rpm). Dissolution media was deaerated and maintained at $37 \pm 0.5^\circ\text{C}$. An aliquot of solution was withdrawn and replaced by an equal volume of fresh medium at the designated times and immediately filtered through a 0.45- μm syringe filter to remove undissolved microparticles. The analytical methods were followed as described above, and the experiments were performed in triplicate.

In vivo Study

Experiment Design

Two open-label BE studies were conducted, which were balanced with two treatments, crossover, single-dose, and a 1-week washout period in twelve healthy subjects. Each study included two formulations: one reference and one of either the test 1 or test 2 formulations. The Chinese Food and Drug Administration (CFDA) and the Institutional Research Ethics Committee of Central South University approved all study protocols. Each participant's sequence was assigned using a computerized random-list generator. Twelve healthy male subjects were administered a single oral dose of the test formulation (test 1 or test 2; 200 mg) and the reference formulation (Celebrex®) under fasted conditions with 240 mL of water in each BE study. Blood samples of 4 mL were collected at 0, 0.5, 1, 1.5, 2, 2.5, 2.75, 3, 3.25, 3.5, 4, 5, 6, 8, 10, 14, 24, and 48 h into heparinized-sodium tubes after dosing. Plasma was separated by centrifugation at 3000 rpm for 10 min and frozen at -20°C until analysis.

Analytical Conditions

Samples from all subjects who received study 1 or study 2 treatment were analyzed. The validated method was used to quantify the plasma concentrations of CEB using HPLC with tandem mass spectrometry methods. Protein was precipitated from the sample extractions by adding acetonitrile, then vortexed for 5 min and centrifuged at $15700 \times g$ for 10 min. The supernatants were collected and then detected using a C18 (4.6×50 mm, 3.5 μm) column (Waters Corp., Milford, MA, USA) maintained at 25°C , with a 5- μL injection volume. A mobile-phase system consisting of 0.1% v/v formic acid in water (component A) and acetonitrile (component B) delivered at a flow rate of 0.6 mL min^{-1} was used to elute the CEB and CEB d_4 (used as internal standards) *via* the following step-gradient program. The mobile phase was maintained at 45% B for 0.3 min, then gradually increased to 98% B over 3.0 min, maintained for 1.0 more minute and brought back to 45% B at 4.1 min, followed by re-equilibration until reaching 5.0 min to the next injection. The negative ions of CEB analytes and CEB d_4 -IS produced by electrospray ion source were measured in multiple reaction-monitoring (MRM) mode with transitions of m/z $380.0 \rightarrow 276.1$ and $384.3 \rightarrow 279.3$ for CEB and CEB d_4 -IS, respectively.

Pharmacokinetic and Statistical Analysis

Pharmacokinetic parameters were calculated using WinNonlin, V.6.1.00 (Pharsight Co., Ltd., USA) based on non-compartmental analysis. Pharmacokinetic parameters such as the area under the plasma concentration *versus* time curve from time 0 to infinity ($\text{AUC}_{0-\infty}$) and the area under the plasma concentration *versus* time curve from time 0 to 48 h ($\text{AUC}_{0-48\text{h}}$) were calculated using the linear trapezoidal rule. The maximum plasma concentration (C_{max}) and the time at which C_{max} was reached (T_{max}) were determined from the individual plasma concentration curves. The pharmacokinetic parameters were analyzed *via* analysis of variance (ANOVA)

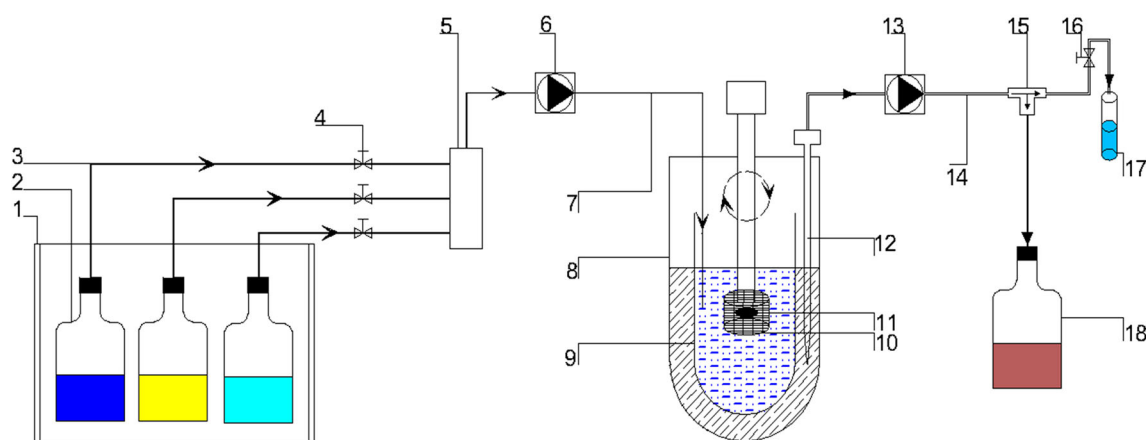


Fig. 1. Schematic diagram of an open-mode two-compartment system dissolution device. 1. Thermostatic waterbath; 2. Media storage bottle; 3. Media pipeline; 4. Infusion control valves; 5. Media selector; 6. High-precision liquid inlet pump; 7. Intake pipe; 8. Acceptor compartment; 9. Donor compartment; 10. Basket; 11. Drug; 12. Sampling needle; 13. High-precision liquid outlet pump; 14. Output pipe; 15. Three-way valve; 16. Sampling control valve; 17. Sample collecting tube; 18. Waste collection bottle

to test the significance among individuals, preparations, and cycles using statistical program for social sciences 21.0 software (SPSS, INC., Chicago, IL, USA). The BE for two formulations was assessed *via* ANOVA for crossover design, and the 90% confidence intervals (CIs) of the test/reference ratio were calculated using log-transformed data.

***In vitro* and *In vivo* Correlation**

To develop the IVIVC with three formulations of different release profiles, the data from both BE studies were combined. Oral CEB plasma profiles were well described with a one-compartment model using the PK module of WinNonlin, V.6.1 (Pharsight Co., Ltd., USA). Without intravenous data, each individual profile was deconvolved to obtain the individual oral fractions *via* the Wagner-Nelson method (25), based on a one-compartment model with first-order elimination, using the following equation:

$$\% \text{ Absorbed} = A_t / A_{\text{final}} = [C_t / K_{\text{el}} + (\text{AUC})_t] \times 100 / (\text{AUC})_{\text{final}} \quad (1)$$

where A_t and A_{final} are the cumulative amounts of the drug absorbed at time (t) and at the final sampling time point. C_t is the plasma concentration at time (t); K_{el} is the elimination rate constant; $(\text{AUC})_t$ and $(\text{AUC})_{\text{final}}$ are the area under the curve from $t=0$ to the time, t , and to the final time. Mean *in vivo* absorbed fractions (F_a , mean) profiles were estimated from the averaged individual *in vivo* absorbed fractions. The absorption rate constant (K_a) was obtained from the least square fitted log-linear plot of the unabsorbed fraction *versus* time (7).

Level A IVIVC was obtained by linear regression between the dissolution fractions (F_{diss} , mean) and absorption fractions (F_a , mean). Mean *in vivo* absorbed fractions with high coefficient of variation (CV%) and individual *in vitro* dissolution fractions obtained from the new dissolution apparatus were processed using several mathematical models including the zero-order, first-order, Higuchi, and Weibull

models. The curves were fitted in Microsoft Excel® (Redmond, WA) with DDSolver, V.1.0 adding (26). Independent measured t test was used to analyze the differences between the mean values of the optimization model *in vitro*.

The simulated plasma profiles *in vivo* were derived from *in vitro* dissolution data using a deconvolution method in which the dissolved fractions (F_{diss} , mean) were used to obtain the corresponding absorbed fractions (F_a , mean) from the established IVIVC (4,27). The concentrations at each time point were obtained using the equation (28):

$$C = \frac{(k_a F X_0)}{V(k_a - k)} \times (e^{-kt} - e^{-k_a t}) \quad (2)$$

where K_a is absorption rate constant calculated from the mean fraction of the absorbed dose, F is the bioavailability, X_0 is the dosage, k is terminal elimination rate constant, and V is the apparent distribution volume. Predicted profiles were used to obtain the predicted $\text{AUC}_{0-\infty}$ and C_{max} . Internal predictability was calculated using Eq. (3) (29,30), and FDA and EMA guidelines validate the IVIVC when the mean prediction error (%PE) in AUC and C_{max} is less than 15% for each individual formulation, and 10% for the mean of all formulations.

Predicted errors (%PE)

$$= \frac{(\text{Observed parameter} - \text{Predicted parameter})}{\text{Observed parameter}} \times 100 \quad (3)$$

RESULTS

***In vitro* Dissolution**

Raw dissolution data obtained from an open-mode dissolution system were a noncumulative-form, and Simpson's rules were used for numerical integration (31).

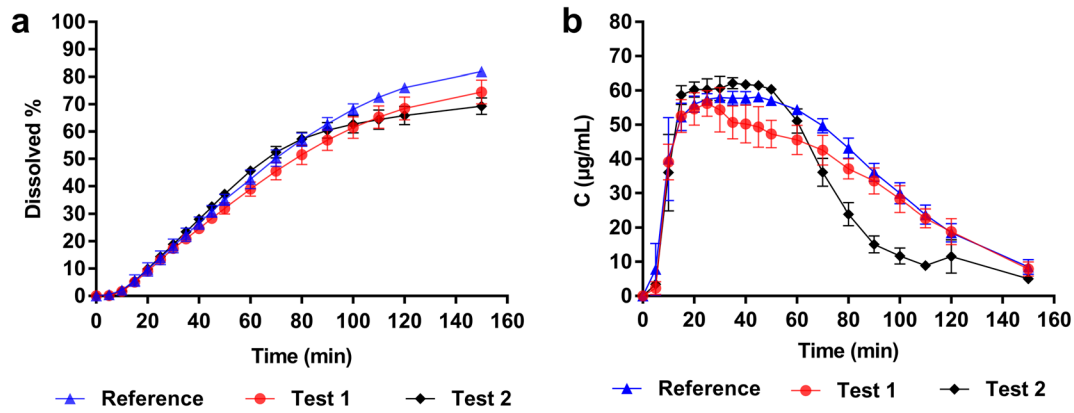


Fig. 2. **a** Accumulative dissolution profiles of CEB formulations (reference product, test 1, and test 2 formulations) using the novel dissolution device in the condition of standard buffers at pH 4.5 containing 0.15% Tween 80, and flow rate of 30 mL/min. **b** Dissolution differential profiles of CEB formulations (reference product, test 1, and test 2 formulations) using the novel dissolution device in the condition of standard buffers at pH 4.5 containing 0.15% Tween 80, flow rate of 30 mL/min. ($n = 6$, mean \pm SD)

Average accumulated dissolved fractions *versus* time of three formulations were obtained *via* the new open-mode two-compartment system dissolution apparatus and are depicted in Fig. 2a. Cumulative release of the reference formulations reached 82% at 2.5 h, whereas test 1 and test 2 were 8–13%

lower than the reference formulations in the condition of pH 4.5 containing 0.15% Tween 80, flow rate of 30 mL/min, and agitation rate of 50 rpm. Furthermore, the differential curve showed that the dissolution rates for all formulations were coincident and plateaued at 30 min, then declined from 60 to 150 min, with each formulation exhibiting a different decreasing tendency (Fig. 2b).

Figure 3a presents the dissolution profiles under sink conditions obtained from the USP II apparatus. CEB almost instantaneously dissolved more than 70% of the dissolution after 30 min. Drug release under non-sink conditions only reached approximately 35% and reached the plateau phase

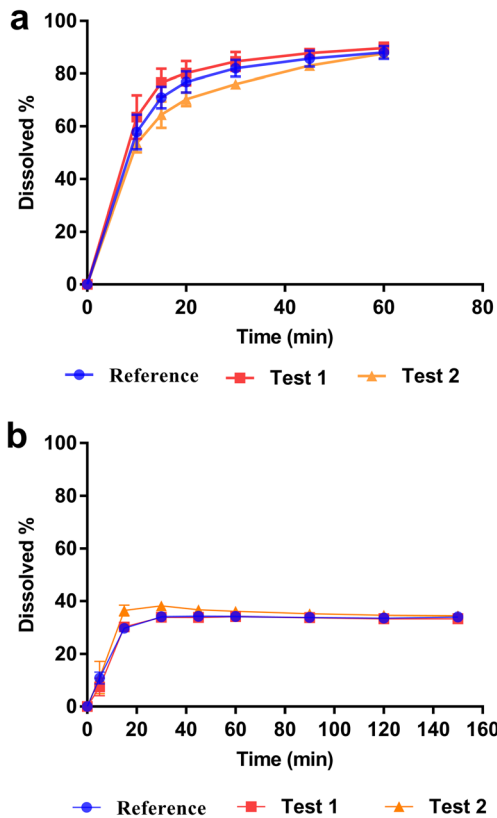


Fig. 3. **a** Dissolution profiles of the CEB formulations (reference product, test 1, and test 2 formulations) under sink conditions (1000 mL tribasic sodium phosphate solution at pH 12 containing 1.0% SDS with a stirring speed of 50 rpm). **b** Dissolution profiles of the CEB formulations (reference product, test 1, and test 2 formulations) under non-sink conditions (1000 mL acetate buffer at pH 4.5 containing 0.15% Tween 80 with a stirring speed of 50 rpm). ($n = 3$, mean \pm SD)

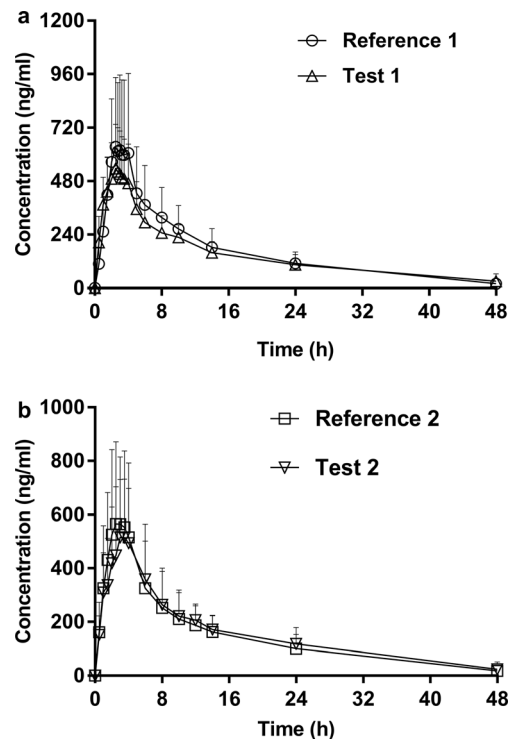


Fig. 4. Mean plasma concentration *vs.* time profiles for both BE studies. **a** Study 1 following a single dose of reference 1, test 1. **b** Study 2 following a single dose of reference 2, test 2. ($n = 12$, mean \pm SD)

Table I. *In vivo* Bioequivalence Results of Study 1 and Study 2. CI: Confidence Interval, BE (Bioequivalent), NBE (Non-bioequivalent), Geo Mean (Geometric Mean), Geo SD (Geometric Standard Deviation). Each Value Is the Mean \pm SD of Twelve Experiments

	Parameter	Ref geo mean	Geo SD	Test geo mean	Geo SD	Geo mean test/ref ration (90%CI)	Equivalence test
Study1 ^a	C _{max}	628.87	1.63	547.12	1.36	87.00 (68.54 to 110.43)	NBE
	AUC _{0-t}	7344.16	1.44	6871.94	1.31	93.57 (82.20 to 106.52)	BE
	AUC _{0-∞}	7625.6	1.46	7602.00	1.43	99.69 (89.80 to 110.67)	BE
Study2 ^b	C _{max}	594.75	1.69	569.12	1.47	95.69 (75.56 to 120.87)	NBE
	AUC _{0-t}	6387.55	1.43	6712.15	1.37	105.08 (93.87 to 117.63)	BE
	AUC _{0-∞}	6678.11	1.41	7152.06	1.46	107.10 (97.05 to 118.18)	BE

^a Stands study 1 included reference 1 and test 1 formulations; ^b Stands study 2 included reference 2 and test 2

within 15 min (Fig. 3b). According to FDA and EMA, the similarity factor (*f*₂) was between 50 and 100 to ensure sameness of the two dissolution profiles (23,32). Dissolution profiles of test 1 and test 2 under sink conditions were compared with the reference, and *f*₂ similarity factor was 69 and 65. The extent of dissolution under non-sink conditions was too low to be evaluated by *f*₂.

$$f_2 = 50 * \text{Log} \left\{ \left[1 + \frac{1}{n} \sum_{t=1}^n (Rt - Tt)^2 \right]^{-0.5} \times 100 \right\} \quad (4)$$

where *n* is the number of time points, and *Rt* and *Tt* are the dissolution value of the reference and test formulation at time *t*.

In vivo Study

Figure 4 shows the average plasma concentration-time profiles of the reference and the test formulations from both BE studies. Table I presents the BE test results for the mean pharmacokinetic parameters of each *in vivo* BE studies. In study 1, the pharmacokinetic end points (C_{max}, AUC_{0-t}, and AUC_{0-∞}) were determined *via* bilateral and unilateral *t* tests. The geometric mean of the test 1/reference 1 ratio yielded the following: 90% confidence interval (CI) of C_{max} (68.54% to 110.43%), AUC₀₋₄₈ (82.20% to 106.52%) AUC_{0-∞} (89.90% to 110.69%). AUC₀₋₄₈ and AUC_{0-∞} were contained entirely within the predefined 80.0% to 125.0% lower and upper limits; for C_{max}, 90% CI was outside the acceptance limits

(80%–125%). In study 2, the geometric mean test 2/reference 2 ratio 90% CI for C_{max} (75.76% to 120.87%), AUC₀₋₄₈ (93.87% to 117.69%), AUC_{0-∞} (97.05% to 118.18%) was observed. The extrapolated C_{max} was 4.24%, with a lower boundary of the 90% CI of C_{max} outside the acceptance limit (80%). Variance analysis showed that the main pharmacokinetic parameters, including LnC_{max}, LnAUC_{0-t}, LnAUC_{0-∞}, T_{1/2}, Cl/F, Vz/F, and MRT, did not differ among subjects and preparations. Thus, according to the FDA, 90% CI was not inside the acceptance limits (80%–125%), and test 1 and test 2 were not considered bioequivalent to the reference Celebrex®. The degree of absorption was the same, but the absorption rates differed.

In vitro and In vivo Correlation

The absorption curve, which was calculated *via* the Wagner-Nelson deconvolution method, displayed completely absorption within 2.5 h for the reference and test 1 preparations, whereas test 2 was absorbed completely within 3 h (Fig. 5). In the first 2 h, the extent of absorption of test 1 and test 2 was higher than that of the reference preparation, then slowed compared with the reference preparation, and the final absorption extents were somewhat consistent over the different time periods.

The level A IVIVC presented a linear correlation between *in vitro* release and *in vivo* absorption (Fig. 6). The equation and linear regression coefficient were F_{abs} = 1.26F_{dis} - 7.21, R² = 0.985 (*p* < 0.01) for the reference formulation, F_{abs} = 1.02F_{dis} + 20.87, R² = 0.994 (*p* < 0.001) for the test 1 formulation, and F_{abs} = 0.98F_{dis} + 13.87, R² = 0.987 (*p* < 0.01) for the test 2 formulation.

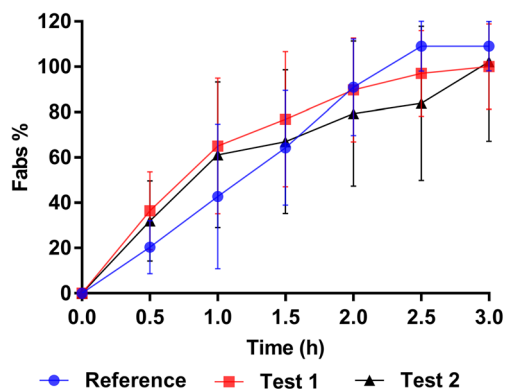


Fig. 5. *In vivo* absorption profiles (oral fraction absorbed [Fabs] versus time) of the CEB formulations (reference, test 1 and test 2) obtained by Wagner-Nelson deconvolution. (*n* = 12, mean \pm SD)

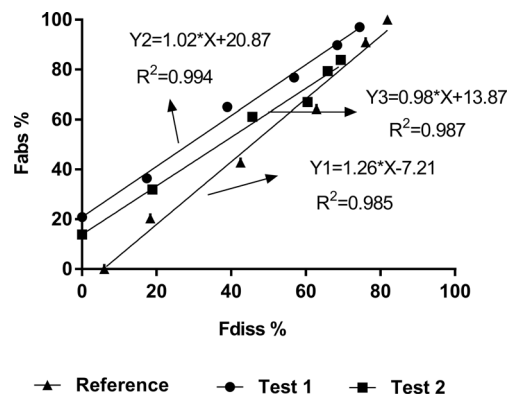


Fig. 6. Level A *in vitro-in vivo* correlation

Table II. The Relevance Between Absorption Rate Constant (K_a), Dissolution Rate Constant (K_{diss}) *In vivo*, and C_{max}

Formulation	K_e (h^{-1})	K_{diss} (h^{-1})	$K_{a, mean}$ (h^{-1})	C_{max} (ng/mL)
Reference 1 ^a	0.11 ± 0.04	1.57 ± 0.25	1.40	699.71 ± 340.52
Reference 2 ^b	0.11 ± 0.04	1.57 ± 0.25	1.40	665.31 ± 301.15
Test 1 ^a	0.12 ± 0.06	0.86 ± 0.16**	1.01	571.70 ± 177.41
Test 2 ^b	0.14 ± 0.07	0.79 ± 0.08**	0.70	608.96 ± 231.84

^a Stands study 1; ^b Stands study 2. ** $P < 0.01$: significantly different from the reference formulation. K_e is elimination rate constant

Table II shows the absorption rate constant (K_a) obtained from the mean *in vivo* absorbed fractions (F_a , mean) and dissolution rate constant (K_{diss}) *in vivo* calculated by the dissolution *in vitro*. The fractions dissolved *in vivo* were estimated from the experimental fractions dissolved *in vitro* through the IVIVC relationship, then, K_{diss} was calculated from the undissolved fraction of the drug. Least square fitted log-linear plot of unabsorbed fraction *versus* time was $Y = 1.40 * X + 0.69$ ($R^2 = 0.8901$) for the reference formulation, $Y = 1.01 * X + 4.65$ ($R^2 = 0.9886$) for the test 1 formulation, and $Y = 0.70 * X + 4.49$ ($R^2 = 0.9748$) for the test 2 formulation. K_{diss} and K_a reflect the dissolution rate and absorption rate *in vivo*, which influenced C_{max} in the pharmacokinetic study.

Tables III and IV summarize the results of the fitted model of the dissolution and absorption profiles, including the parameters. The optimization model was determined by Akaike's information criterion (AIC) (33) and the determination coefficient (R^2) which represents the goodness of fit, indicating the closeness of the model for fitting the dissolution and absorption process. Dissolution kinetics of the reference and all test formulations failed to meet the Higuchi model ($R^2 < 0.9$, $AIC > 142$). The Weibull and first-order models well described the dissolution process *in vitro*, but Weibull was better ($R^2 > 0.99$) with minimum AIC. The absorption kinetics of the reference preparation conformed to the zero-order rate model, with parameters, $k_0 = 0.732\%$ /min, $R^2 = 0.9967$, and $AIC = 16.14$. For the test 1 and test 2 preparations, according to AIC value, the absorption kinetics coincided with the Weibull model with $\alpha = 112.11$,

54.27, $\beta = 1.16$, 0.93, and the first-order model with $k_1 = 0.017 \text{ min}^{-1}$, 0.013 min^{-1} .

Table V summarizes the internal validations. Prediction error percentages (PE%) of C_{max} and AUC were obtained by comparing with the observed and predicted values. Figure 7 shows the observed and predicted plasma profiles.

DISCUSSION

CEB is a BCS II drug with dissolution being its limiting factor for absorption *in vivo*, making it a good candidate for developing an IVIVC. Dissolution profiles under non-sink conditions were almost superimposable and the release amount was lower than that of the novel device method. Owing to the lack of an open-loop configuration, which can achieve the absorptive sink condition by increasing the dissolution media volume, a low level of drug release was observed. Dissolution plateaued at 15 min and there was no *in vitro-in vivo* correlation with real dissolution *in vivo*. Under the sink conditions, the dissolution profiles of the formulation were similar in tribasic sodium phosphate solution with 1.0% SDS, which is recommended by the FDA, because CEB is insoluble at a physiological pH value (3.2 mg/L at pH 4.5). However, this method significantly deviates from biological conditions (34), and using high-level surfactants would lead to the indistinguishable dissolution behaviors (35). No discrimination was observed between formulations under either non-sink conditions or sink conditions. A conventional one-compartment, closed-environment dissolution setup has limitations to develop a discriminative method and establish

Table III. Release Kinetic *In vitro* Parameters as well as Correlation Coefficients and Akaike's Information Criterion of Each Equation for Celecoxib

Equation	Formulations	Parameter	R^2	AIC	
Zero-order $F = k_0 * t$	Reference	$K_0 = 0.65 \pm 0.01$	0.9687	117.670	
	Test 1	$K_0 = 0.58 \pm 0.03$	0.9692	110.840	
	Test 2	$K_0 = 0.59 \pm 0.03$	0.9142	132.370	
First-order $F = 100 * [1 - \text{Exp}(-k_1 * t)]$	Reference	0.01 ± 0.0003	0.9579	122.884	
	Test 1	0.01 ± 0.001	0.9670	112.689	
	Test 2	0.01 ± 0.001	0.9651	115.358	
Higuchi $F = kH * t^{0.5}$	Reference	$kH = 5.92 \pm 0.12$	0.8384	148.900	
	Test 1	$kH = 5.28 \pm 0.31$	0.8343	143.540	
	Test 2	$kH = 5.49 \pm 0.25$	0.8538	142.640	
Weibul $F = 100 * [1 - \text{Exp}(-(t^\beta) / \alpha)]$	Reference	$\alpha = 561.54 \pm 172.72$	$\beta = 1.40 \pm 0.08$	0.9973	70.030
	Test 1	$\alpha = 445.65 \pm 112.41$	$\beta = 1.30 \pm 0.07^*$	0.9946	78.330
	Test 2	$\alpha = 224.19 \pm 39.16^*$	$\beta = 1.16 \pm 0.05^*$	0.9751	110.560

Each value is the mean ± SD of six experiments. * $P < 0.05$: significantly different from the reference formulation

Table IV. Absorption Kinetic *In vivo* Parameters as well as Correlation Coefficients and Akaike's Information Criterion of Each Equation for Celecoxib

Equation	Formulations	Parameter	R ²	AIC	
Zero-order F = k ₀ *t	Reference	K ₀ = 0.73	0.9967	16.14	
	Test 1	K ₀ = 0.75	0.8627	42.96	
	Test 2	K ₀ = 0.66	0.8260	42.80	
First-order F = 100*[1-Exp(-k ₁ *t)]	Reference	K ₁ = 0.013	0.8874	43.31	
	Test 1	K ₁ = 0.017	0.9931	25.02	
	Test 2	K ₁ = 0.013	0.9897	25.81	
Higuchi F = kH*t ^{0.5}	Reference	kH = 7.52	0.8748	36.95	
	Test 1	kH = 8.01	0.9895	27.51	
	Test 2	kH = 7.07	0.9812	29.45	
Weibul F = 100*[1-Exp[-(t ^β)/α]]	Reference	α = 5239.64	β = 1.95	0.9705	37.26
	Test 1	α = 112.11	β = 1.16	0.9972	21.66
	Test 2	α = 54.27	β = 0.93	0.9912	26.91

IVIVC because of the lack of biorelevance (17). Open-loop configurations enable increasing analyte dissolution without high-level surfactants or other solvents in the dissolution media (36). The characteristic of open-loop system is to mimic the gastrointestinal tract by continuously extracting drug from the acceptor vessel and thus is analogous to the dissolution-absorption dynamic process.

In the new open-mode two-compartment system dissolution device, the time for investigating dissolution behavior was extended to 2.5 h, which was consistent with the time needed to reach the maximum fraction of the absorbed dose of CEB (37). Importantly, the differential curves were obtained to determine the changes in dissolution rate. The differential curves showed that the dissolution rates between all formulations were coincident for 30 min because the capsules disintegrated slowly with low rotational speeds and a small solvent volume. Once dissolution rates plateaued at 30 min, the decreasing dissolution rates in test 1 and test 2 were faster than that of the reference. Consequently, the cumulative dissolution was less than that of the reference (Fig. 2a) because the SDS content in the test and reference formulations differed. Figure 2a indicates an incomplete cumulative release at approximately 70–80% for all formulations under the selected conditions, which likely reflected *in vivo* dissolution and limited CEB absorption because the extent of dissolution *in vitro* was limited by the solubility and the fixed volume of the media available. *In vivo*, sink conditions were generated by the high permeability (absolute bioavailability of CEB was approximately 80% (38)); thus,

the limit factor of absorption was transferred from the solubility of the compound to its dissolution rate (19). In the novel device, the amount of drug in the removal medium simulated the extent of the absorbed dose; that is, faster dissolution rates required faster flow rates. Flow rates and surfactants simultaneously affect dissolution profiles of CEB. No discrimination occurred between formulations under a high flow rate and high-level surfactant, and the total amount released was less than 80%. Shi *et al.* applied biphasic dissolution device to examine release profiles of celecoxib formulations in which the flow rate of the pump (USP IV system) was set at 30 mL/min (16). Two-compartment setup was modified based on the mini-paddle apparatus with a scaled down geometrically dimension, and high agitation is disadvantageous for establishing IVIVC (39). The dissolution medium volume is usually 250 mL, with a paddle revolution speed of 50 rpm (40). Furthermore, surfactants played a major role in solubilizing the preparations, and a lower Tween 80 concentration was used to achieve a better *in vitro* and *in vivo* correlation (37). The C_{max} of the differential curves was approximately 60 µg/mL (Fig. 2b), which was near the celecoxib solubility (46.2 µg/mL) at the fasted state simulated intestinal fluid (FaSSIF) medium (19).

In this study, the new dissolution method offered a discriminative dissolution profiles (Fig. 2). Test 1 and test 2 were 8–13% lower than the reference formulation over 60–150 min, and the release rates were slow with no momentum over 2.5 h. The values of f₂ were 67 and 59 respectively comparing reference formulation *versus* test 1 and test 2

Table V. Prediction Errors of C_{max} and AUC_{0-∞} Values from the Developed *In vitro-In vivo* Correlation

Validation	Formulation	C _{max} (ng ml ⁻¹)			AUC _{0-∞} (ng h ml ⁻¹)		
		Observed	Predicted	PE%	Observed	Predicted	PE%
Internal	Reference ^a	699.71	585.60	16.31	8190.31	7372.38	9.99
	Test 1	571.70	532.57	6.84	8121.46	7397.91	8.91
	Test 2	608.96	525.33	13.73	7403.78	7430.82	2.84
Average internal				12.29			7.25

^a Prefers study 1

formulations. Although dissolution profiles are similar in terms of the f2 rule, it was not suitable for the dissolution profiles obtained by the new apparatus.

As shown in Table II, when the elimination rate constant remained unchanged, K_{diss} and K_a of test 1 and test 2 *in vivo* were smaller than K_{diss} and K_a *in vivo* of the reference 1 in study 1 and study 2. This trend was consistent with the C_{max} - K_{diss} *in vivo* which showed significant differences between test 1 and the reference formulations and between test 2 and the reference formulations ($p < 0.01$). The BE results showed that the test 1 and test 2 formulations were not bioequivalent to the reference formulation because the C_{max} was lower than the reference formulation (Fig. 4). We determined the standard of dissimilar dissolution curves: the test formulation release rate was lower or faster than that of the reference formulation at 60–150 min with a different K_{diss} value *in vivo*, which may have led to the lack of bioequivalence of C_{max}

(41). This trend was consistent with the absorption fraction (Fig. 5) and BE results. A linear correlation between the *in vitro* release and *in vivo* absorption indicated that the slope of the correlation between dissolution *in vitro* and absorption *in vivo* was well established. The correlation models had R^2 values of >0.98 ($p < 0.01$) and the linear regression coefficients indicated a good IVIVC, with a higher correlation coefficient. The concept of the correlation level is depended on the ability of the correlation to reflect the complete plasma drug level-time profile (1). A level A correlation is crucial and reveals a point-to-point relationship between the *in vitro* dissolution and the *in vivo* input rate, and the measurement of the *in vitro* dissolution rate alone can sufficiently determine the biopharmaceutical rate of the dosage form (42,43).

In vitro release and *in vivo* absorption were fitted by the Weibull equation and first-order equation for the test formulations, of which, the zero-order rate model better described the absorption kinetics of the reference preparation. Parameters α and β *in vitro* differed between test 2 and the reference formulations, and significant differences ($p < 0.05$) were observed. However for test 1, α was not considered statistically significant ($p > 0.05$), β ($p < 0.05$). β typically determines the curve shape, and for $\beta = 1$, the curves' exponential function types were S type for $\beta > 1$ and a parabolic type for $\beta < 1$ (44). The β values of the dissolution and absorption curves were ≥ 1 , indicating that the shapes of the curves *in vivo* and *in vitro* were more consistent. The scale parameter of α had the function of magnification or reduction. For the test 1 and test 2 formulations, a time scale factor value was 4-fold that of the factor being estimated by linear fitting of both the *in vitro* release and the *in vivo* absorption profiles using the Weibull function (27,45). This indicates that the new dissolution method could be expected to use as a quality control tool to distinguish preparation differences to some extent, while the USP II dissolution method cannot discriminate preparations.

The pharmacokinetic parameters investigated in the *in vivo* studies (supplemental Table 1) were consistent with those in the literature reports (46). CEB was slowly absorbed with a T_{max} of 2–3 h when given orally in a solid form, and the main absorption sites included the duodenum, jejunum, and colon (47). Dissolution from the celecoxib capsules in the stomach is not reported to play an important role in the intestinal absorption of celecoxib (19). The plasma concentrations-time profiles (Fig. 7) indicate that the predicted results concurred with the *in vivo* profile with an excellent predictability for the final IVIVC model. The $\text{AUC}_{0-\infty}$ prediction errors were within the accepted limits (15% for the individual formulations and 10% for the average formulations). However, for the reference formulation, C_{max} prediction errors were more than 15%. This was unsurprising, because high standard deviations in the *in vivo* study (plasma concentrations) lead to distinction between the $C_{\text{max,mean}}$ and the maximum plasma concentration of the average plasma concentration-time profiles. Nevertheless, the results showed a good correlation *in vitro* and *in vivo* as well as discriminations between different formulations were observed. Pharmaceutical companies can use the novel

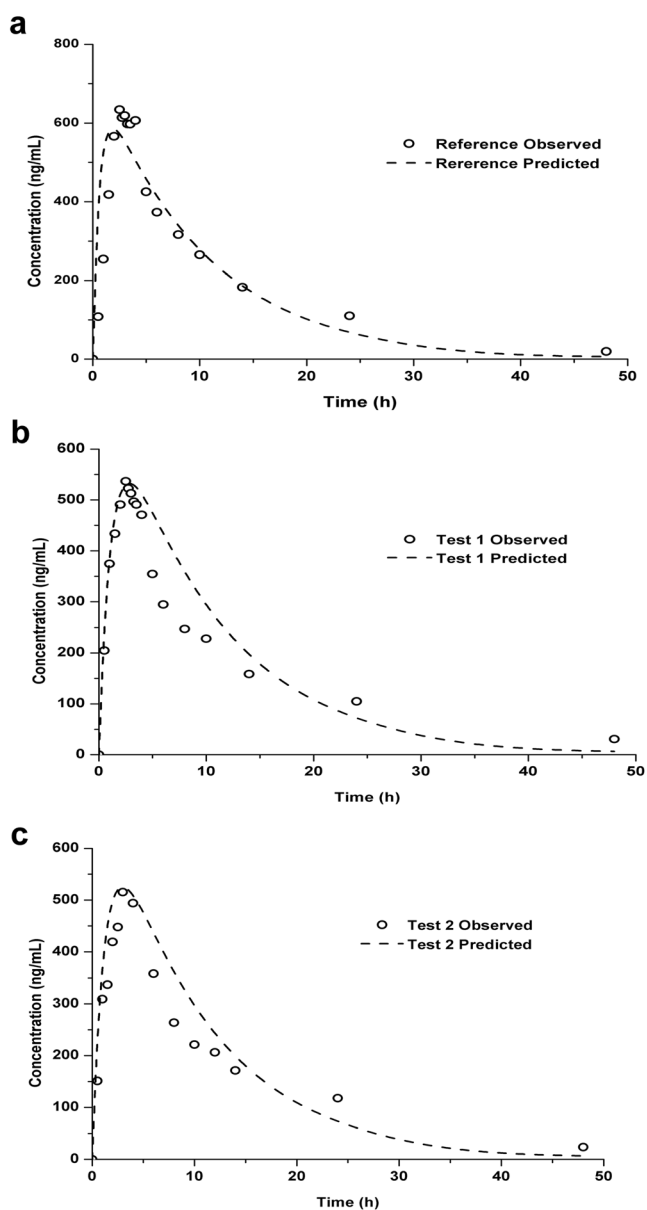


Fig. 7. Observed and predicted CEB plasma profiles for the three studied formulations

dissolution method to assess the *in vivo* predictive value for the formulation selection before *in vivo* studies.

IVIVC is widely used as a risk analysis tool to select formulations and reduce time and costs in BE trials. Establishing a good IVIVC requires physiological dissolution devices and media. This new model discriminates the suitable difference for the formulations *in vitro* dissolution and predicts profiles *in vivo* after establishing an IVIVC. Two-compartment system may offer advantages for the poorly soluble drugs with limited solubility compared with USP II methods. It is also suitable for extended release forms with a pH shift that simulates gastric dissolution followed by intestinal dissolution and absorption. The dissolution data and IVIVC model can be used as a tool to modify the reformulation process and to make *in vivo* predictions for further bioequivalence trials.

Moreover, there are some drawbacks that cannot be ignored. More time and solvent are consumed when performing dissolution tests of CEB in a two-compartment system device. At present, this device has only been used for CEB research, and use of different drug compounds and dissolution media requires further study.

CONCLUSION

This work demonstrated that an open-mode two-compartment system dissolution device was useful for evaluating formulation performances of poorly water-soluble drugs compared with traditional methods. Donor and acceptor compartments in the novel apparatus simulate drug dissolution and absorption in the gastrointestinal tract. Four dissolution-kinetics models were used to fit the absorption and dissolution kinetics, of which, the Weibull equation had the best fitting effect except that the absorption of the reference preparation satisfied zero-order kinetics. Level A correlations with good correlation coefficients were successfully established by combining data from different BE studies of IR CEB products. *In vitro* dissolution correlated well with *in vivo* absorption and enabled predicting the *in vivo* plasma concentration-time profiles of CEB, which may need further refinement to fulfill regulatory requirements for a biowaiver claim.

ACKNOWLEDGMENTS

This research was supported by Hunan Huize Biopharmaceutical Co., Ltd., and Hunan Taixin Pharmaceutical Technology Co., Ltd.

COMPLIANCE WITH ETHICAL STANDARDS

Conflict of Interest The authors declare that they have no conflicts of interest.

REFERENCES

- Emami J. In vitro - in vivo correlation: from theory to applications. *J Pharm Pharm Sci.* 2006;9(2):169–89.
- Deng J, Staufenbiel S, Hao S, Wang B, Dashevskiy A, Bodmeier R. Development of a discriminative biphasic in vitro dissolution test and correlation with in vivo pharmacokinetic studies for differently formulated racecadotril granules. *J Control Release.* 2017;255:202–9. <https://doi.org/10.1016/j.jconrel.2017.04.034>.
- FDA US. Guidance for industry: dissolution testing of immediate-release solid oral dosage forms. Food and Drug Administration, Center for Drug Evaluation and Research(CDER). 1997.
- Gonzalez-Garcia I, Mangas-Sanjuan V, Merino-Sanjuan M, Alvarez-Alvarez C, Diaz-Garzon Marco J, Rodriguez-Bonnin MA, et al. IVIVC approach based on carbamazepine bioequivalence studies combination. *Pharmazie.* 2017;72(8):449–55. <https://doi.org/10.1691/ph.2017.7011>.
- Kim TH, Bulitta JB, Kim DH, Shin S, Shin BS. Novel extended in vitro-in vivo correlation model for the development of extended-release formulations for baclofen: from formulation composition to in vivo pharmacokinetics. *Int J Pharm.* 2019;556:276–86. <https://doi.org/10.1016/j.ijpharm.2018.12.007>.
- Tietz K, Gutknecht SI, Klein S. Predicting local drug availability of locally acting lozenges: from method design to a linear level A IVIVC. *Eur J Pharm Biopharm.* 2018;133:269–76. <https://doi.org/10.1016/j.ejpb.2018.10.015>.
- Jacob S, Nair AB. An updated overview with simple and practical approach for developing in vitro-in vivo correlation. *Drug Dev Res.* 2018;79(3):97–110. <https://doi.org/10.1002/ddr.21427>.
- Kataoka M, Yano K, Hamatsu Y, Masaoka Y, Sakuma S, Yamashita S. Assessment of absorption potential of poorly water-soluble drugs by using the dissolution/permeation system. *Eur J Pharm Biopharm.* 2013;85(3 Pt B):1317–24. <https://doi.org/10.1016/j.ejpb.2013.06.018>.
- Higuchi M, Nishida S, Yoshihashi Y, Tarada K, Sugano K. Prediction of coning phenomena for irregular particles in paddle dissolution test. *Eur J Pharm Sci.* 2015;76:213–6. <https://doi.org/10.1016/j.ejps.2015.05.019>.
- Gray VA. Pharmaceutical analysis | dissolution testing. In: Worsfold P, Poole C, Townshend A, Miró M, editors. *Encyclopedia of analytical science.* Third ed. Oxford: Academic Press; 2019. p. 182–7.
- Hate SS, Reutzel-Edens SM, Taylor LS. Absorptive dissolution testing of supersaturating systems: impact of absorptive sink conditions on solution phase behavior and mass transport. *Mol Pharm.* 2017;14(11):4052–63. <https://doi.org/10.1021/acs.molpharmaceut.7b00740>.
- Delalonde M, Ruiz T. Dissolution of pharmaceutical tablets: the influence of penetration and drainage of interstitial fluids. *Chem Eng Process.* 2008;47(3):370–6. <https://doi.org/10.1016/j.cep.2007.01.003>.
- Park K. Absence of in vivo-in vitro correlation in per-oral drug delivery. *J Control Release.* 2014;180:150. <https://doi.org/10.1016/j.jconrel.2014.03.020>.
- Lee C-M, Luner PE, Locke K, Briggs K. Application of an artificial stomach-duodenum reduced gastric pH dog model for formulation principle assessment and mechanistic performance understanding. *J Pharm Sci.* 2017;106(8):1987–97. <https://doi.org/10.1016/j.xphs.2017.02.015>.
- Mizoguchi M, Kataoka M, Yokoyama K, Aihara R, Wada K, Yamashita S. Application of an in vitro dissolution/permeation system to early screening of oral formulations of poorly soluble, weakly basic drugs containing an acidic pH-modifier. *J Pharm Sci.* 2018;107(9):2404–10. <https://doi.org/10.1016/j.xphs.2018.05.009>.
- Shi Y, Gao P, Gong Y, Ping H. Application of a biphasic test for characterization of in vitro drug release of immediate release formulations of celecoxib and its relevance to in vivo absorption. *Mol Pharm.* 2010;7(5):1458–65. <https://doi.org/10.1021/mp100114a>.
- Phillips DJ, Pygall SR, Cooper VB, Mann JC. Overcoming sink limitations in dissolution testing: a review of traditional methods and the potential utility of biphasic systems. *J Pharm Pharmacol.* 2012;64(11):1549–59. <https://doi.org/10.1111/j.2042-7158.2012.01523.x>.
- Fotaki N, Symillides M, Reppas C. In vitro versus canine data for predicting input profiles of isosorbide-5-mononitrate from oral extended release products on a confidence interval basis. *Eur J Pharm Sci.* 2005;24(1):115–22. <https://doi.org/10.1016/j.ejps.2004.10.003>.

19. Shono Y, Jantravid E, Janssen N, Kesisoglou F, Mao Y, Vertzoni M, et al. Prediction of food effects on the absorption of celecoxib based on biorelevant dissolution testing coupled with physiologically based pharmacokinetic modeling. *Eur J Pharm Biopharm.* 2009;73(1):107–14. <https://doi.org/10.1016/j.ejpb.2009.05.009>.
20. Yazdani M, Briggs K, Jankovsky C, Hawi A. The “high solubility” definition of the current FDA Guidance on Biopharmaceutical Classification System may be too strict for acidic drugs. *Pharm Res.* 2004;21(2):293–9.
21. Gangadharappa HV, Chandra Prasad SM, Singh RP. Formulation, in vitro and in vivo evaluation of celecoxib nanosponge hydrogels for topical application. *J Drug Deliv Sci Technol.* 2017;41:488–501. <https://doi.org/10.1016/j.jddst.2017.09.004>.
22. Mudie DM, Murray K, Hoad CL, Pritchard SE, Garnett MC, Amidon GL, et al. Quantification of gastrointestinal liquid volumes and distribution following a 240 mL dose of water in the fasted state. *Mol Pharm.* 2014;11(9):3039–47. <https://doi.org/10.1021/mp500210c>.
23. Kostewicz ES, Abrahamsson B, Brewster M, Brouwers J, Butler J, Carlet S, et al. In vitro models for the prediction of in vivo performance of oral dosage forms. *Eur J Pharm Sci.* 2014;57:342–66. <https://doi.org/10.1016/j.ejps.2013.08.024>.
24. Kakhi M. Classification of the flow regimes in the flow-through cell. *Eur J Pharm Sci.* 2009;37(5):531–44. <https://doi.org/10.1016/j.ejps.2009.04.003>.
25. Wagner JG, Nelson E. Kinetic analysis of blood levels and urinary excretion in the absorptive phase after single doses of drug. *J Pharm Sci.* 1964;53(11):1392–403. <https://doi.org/10.1002/jps.2600531126>.
26. Zhang Y, Huo M, Zhou J, Zou A, Li W, Yao C, et al. DDSolver: an add-in program for modeling and comparison of drug dissolution profiles. *AAPS J.* 2010;12(3):263–71. <https://doi.org/10.1208/s12248-010-9185-1>.
27. Ruiz Picazo A, Martinez-Martinez MT, Colon-Useche S, Iriarte R, Sanchez-Dengra B, Gonzalez-Alvarez M, et al. In vitro dissolution as a tool for formulation selection: Telmisartan two-step IVIVC. *Mol Pharm.* 2018;15(6):2307–15. <https://doi.org/10.1021/acs.molpharmaceut.8b00153>.
28. Asmanova N, Koloskov G, Ilin AI. Coupled solutions of one- and two-compartment pharmacokinetic models with first-order absorption. *J Pharmacokinet Pharmacodyn.* 2013;40(2):229–41. <https://doi.org/10.1007/s10928-013-9312-6>.
29. EMA. Guideline on quality of oral modified release products. 2014.
30. FDA. Guidance for industry: extended release oral dosage forms: development, evaluation and application of in vitro/in vivo correlations. Food and Drug Administration, Rockville, MD. 1997.
31. Misra S, Wahab MF, Patel DC, Armstrong DW. The utility of statistical moments in chromatography using trapezoidal and Simpson's rules of peak integration. *J Sep Sci.* 2019;42(8):1644–57. <https://doi.org/10.1002/jssc.201801131>.
32. Costa P, Sousa Lobo JM. Modeling and comparison of dissolution profiles. *Eur J Pharm Sci.* 2001;13(2):123–33.
33. Vrieze SI. Model selection and psychological theory: a discussion of the differences between the Akaike information criterion (AIC) and the Bayesian information criterion (BIC). *Psychol Methods.* 2012;17(2):228–43. <https://doi.org/10.1037/a0027127>.
34. Nicolaides E, Galia E, Efthymiopoulos C, Dressman JB, Reppas C. Forecasting the in vivo performance of four low solubility drugs from their in vitro dissolution data. *Pharm Res.* 1999;16(12):1876–82. <https://doi.org/10.1023/a:1018959511323>.
35. Dressman JB, Reppas C. In vitro-in vivo correlations for lipophilic, poorly water-soluble drugs. *Eur J Pharm Sci.* 2000;11(Suppl 2):S73–80.
36. Posti J, Speiser PP. Sink conditions in the flow-through cell during dissolution. *Int J Pharm.* 1980;5:101–7.
37. Wang F, Barnes TJ, Prestidge CA. Celecoxib confinement within mesoporous silicon for enhanced oral bioavailability. *Mesoporous Biomaterials.* 2014;1(1). <https://doi.org/10.2478/mesbi-2013-0001>.
38. Paulson SK, Hribar JD, Liu NW, Hajdu E, et al. Metabolism and excretion of [(14)C] celecoxib in healthy male volunteers. *Drug Metab Dispos.* 2000;28:308–14.
39. Levy G, Leonards JR, Procknal JA. Interpretation of in vitro dissolution data relative to the gastrointestinal absorption characteristics of drugs in tablets. *J Pharm Sci.* 1967;56(10):1365–7. <https://doi.org/10.1002/jps.2600561039>.
40. Klein S, Shah VP. A standardized mini paddle apparatus as an alternative to the standard paddle. *AAPS PharmSciTech.* 2008;9(4):1179–84. <https://doi.org/10.1208/s12249-008-9161-6>.
41. Schall R, Luus HG, Steijnans VW, Hauschke D. Choice of characteristics and their bioequivalence ranges for the comparison of absorption rates of immediate-release drug formulations. *Int J Clin Pharmacol Ther.* 1994;32(7):323–8.
42. Kakhi M, Suarez-Sharp S, Shepard T, Chittenden J. Application of an NLME–stochastic deconvolution approach to level A IVIVC modeling. *J Pharm Sci.* 2017;106(7):1905–16. <https://doi.org/10.1016/j.xphs.2017.03.015>.
43. Li ZQ, He X, Gao X, Xu YY, Wang YF, Gu H, et al. Study on dissolution and absorption of four dosage forms of isosorbide mononitrate: level A in vitro-in vivo correlation. *Eur J Pharm Biopharm.* 2011;79(2):364–71. <https://doi.org/10.1016/j.ejpb.2011.04.015>.
44. Cupera J, Lansky P, Sklubalova Z. Sampling times influence the estimate of parameters in the Weibull dissolution model. *Eur J Pharm Sci.* 2015;78:171–6. <https://doi.org/10.1016/j.ejps.2015.07.015>.
45. Cardot JM, Lukas JC, Muniz P. Time scaling for in vitro-in vivo correlation: the inverse release function (IRF) approach. *AAPS J.* 2018;20(6):95. <https://doi.org/10.1208/s12248-018-0250-5>.
46. Park MS, Shim WS, Yim SV, Lee KT. Development of simple and rapid LC-MS/MS method for determination of celecoxib in human plasma and its application to bioequivalence study. *J Chromatogr B.* 2012;902:137–41. <https://doi.org/10.1016/j.jchromb.2012.06.016>.
47. Paulson SK, Vaughn MB, Jessen SM, Lawal Y, Gresk CJ, Yan B, et al. Pharmacokinetics of celecoxib after oral administration in dogs and humans: effect of food and site of absorption. *J Pharmacol Exp Ther.* 2001;297(2):638–45.